ChemComm
Chemical Communications

Accepted Manuscript

This article can be cited before page numbers have been issued, to do this please use: Z. Li, J. Zhang, X. Tian and N. Ding, *Chem. Commun.*, 2019, DOI: 10.1039/C9CC04714J.

ROYAL SOCIETY OF CHEMISTRY

rsc.li/chemcomm

View Article Online
DOI: 10.1039/C9CC04714J

COMMUNICATION

A novel hydrosoluble near-infrared fluorescence probe for specifically monitoring of tyrosinase and application in a mouse model

Received 00th January 20xx,
Accepted 00th January 20xx

DOI: 10.1039/x0xx00000x

Jiahang Zhang, Zhao Li*, Xinwei Tian, and Ning Ding

A novel hydrosoluble near-infrared (NIR) fluorescence probe that could specifically identify tyrosinase has been successfully constructed and applied to imaging of tyrosinase in living cells and zebrafish. Notably, the probe has been successfully applied to the diagnosis of melanoma in a xenogeneic mouse model.

Melanoma, an aggressive malignancy cutaneous, is the most deadly skin cancer, and its morbidity has increased rapidly in the past decades.[1] Tyrosinase (TYR, EC 1.14.18.1), a copper-containing monooxygenase, can catalyze the oxidation of tyramine or tyrosine into quinones which triggers melanin formation.[2] Melanin plays a key role in the development of melanoma.[3] What's more, excessive expression of TYR in melanoma cancer cells is used as an independent biomarker for the diagnosis and prognosis of melanoma.[4] Consequently, it arises out of profound significance to detect TYR simply and accurately for both fundamental research in biological systems and practical applications in clinical diagnosis of melanoma.

Up to present, there have been numerous traditional detection methods for TYR, such as colorimetric and electrochemical assay.[5,6] Fluorescent probes are definitely a better choice for more convenient, effective, and accurate detection of TYR.[7] For *in vivo* imaging studies, near-infrared (NIR) fluorescent probes are more desired because they have excellent tissue penetration, low biological and autofluorescence damage.[8] Especially, the combination of NIR fluorescent probe and confocal imaging has attracted widespread attention for monitoring TYR in living biological systems. Nevertheless, most of the current fluorescent probes are interfered by some reactive oxygen species (ROS) such as HOCl, H_2O_2 and $ONOO^-$, to generate fluorescence response similar to TYR reaction.[9] In order to solve this problem, we have adopted a new TYR recognition fragment, 3-hydroxybenzyloxy, which can specifically identify TYR instead of ROS.[10] The decomposed product of the unstable precursor cyanine dyes not only shows high stability but also preserves the characteristic of near-infrared fluorescence emission of cyanine dyes.[11] In view of that, we chose the IR-783 that have excellent near-infrared spectroscopic feature and good water solubility due to the existence of sulfonic acid group.

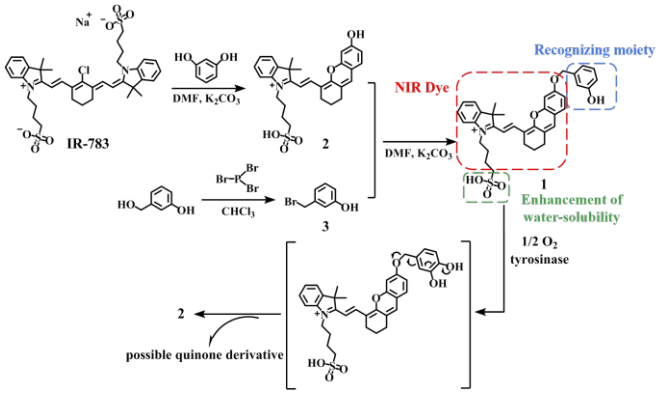

Scheme 1 Synthesis of probe **1** and its reaction with TYR.

In this paper, we successfully designed and synthesized a hydrosoluble, selective, sensitive and reliable NIR fluorescence probe, (*E*)-2-(2-(6-((3-hydroxybenzyl)oxy)-2,3-dihydro-1*H*-xanthen-4-yl)vinyl)3,3-dimethyl-1-(4-sulfobutyl)-3*H*-indol-1 ium (**1**), for the detection of TYR activity. The presence of TYR will cut off the bonds that connect fluorophore with recognize moiety in the probe, resulting in the release of the fluorophore, which has reached the purpose of detecting TYR (Scheme 1). The probe **1** indeed exhibits excellent properties, which applies to the detection of endogenous TYR in living cells and zebrafish. Notably, the probe has been successfully applied to the diagnosis of melanoma in a xenogeneic mouse model. Detailed characterization of fluorophore **2** and probe **1** were described in Fig. S1-S4 (ESI†).

After synthesized and was characterized by ^1H NMR, ^{13}C NMR, and ESI-MS, which demonstrated the successful synthesis of the probe **1**. The UV-visible absorption and fluorescence spectra of probe **1** in the absence and presence of TYR were shown in Fig.1 A and B. Initially, the probe **1** had the absorption maximum at 600 nm. After reaction with TYR, the maximum absorption peak was around 670 nm (Fig. 1A). As shown in Fig. 1B, with the added amount of

Shaanxi Engineering Laboratory for Food Green Processing and safety Control, College of Food Engineering and Nutritional Science, Shaanxi Normal University, Xi'an 710062, China. E-mail: lizhao0309@snnu.edu.cn.
Electronic Supplementary Information (ESI) available: Apparatus and reagents, and other supporting data. See DOI: 10.1039/x0xx00000x

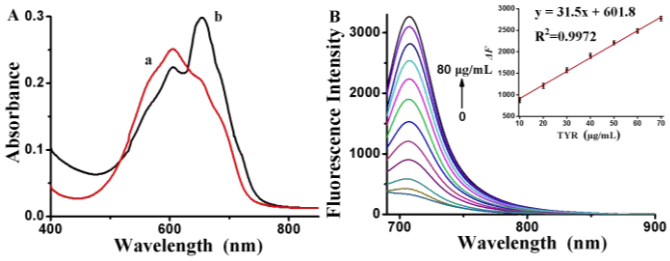

Fig. 1 (A) Absorption spectra of probe **1** (10 μM) (a) before and (b) after reaction with TYR (80 μg/mL). (B) Fluorescence spectra of probe **1** (10 μM) reacting with TYR at different concentrations (0, 2, 5, 8, 10, 20, 30, 40, 50, 60, 70 and 80 μg/mL). The linear fitting curve of ΔF towards the concentration of TYR between 10-70 μg/mL. ΔF is the fluorescence enhancement of probe **1** at 708 nm with and without TYR. The reaction was performed in 10 mM PBS at 37 °C for 3 h. λex/em = 670/708 nm.

TYR increased, probe **1** showed gradual enhanced fluorescence signal with a peak at 708 nm. It is worth noting that the absorption and fluorescence spectra of the reaction system are similar to those of fluorophore **2**, with a quantum yield of 0.18, indicating that the free fluorophore **2** is caused by the cleavage reaction triggered by TYR (Scheme 1). The formation of fluorophore **2** was further verified by electrospray ionization mass spectral analysis (m/z 506.19 $[M]^+$; Fig. S5, ESI†).

To optimize the detection condition, a series of experiments related to factors such as reaction incubation time, pH and temperature were carried out. The incubation time had a remarkable influence on the fluorescence intensity, and this parameter should be determined at the beginning of the reaction. Kinetic curves were clearly from Fig. S6 (ESI†), the fluorescent intensity of the reaction solution increased rapidly and almost reached the platform in about 3 h. It indicated that the reaction was complete after 3 h. Hence, we chose 3 h as the optimal response time. In addition, the fluorescence of the probe **1** (control) does not change significantly during the same period of time, which fully reflects the high stability of the probe in the detection system. It was observed in Fig. S7 (ESI†) that the fluorescence intensities of probe **1** stayed almost constant in the pH range from 5.0 to 8.0 and temperature from 25 to 42 °C, indicating its high stability. After reaction with TYR, the fluorescence intensities of probe **1** changed significantly with the increase of pH from 5.0 to 8.0. Similarly, the fluorescence of the reaction solution reached its maximum at a temperature of 37 °C (Fig. S8, ESI†). According to the results, we preferred pH = 7.4 and 37 °C as the best conditions. Together, these *in vitro* results indicated that probe **1** exhibits a great stability in the absence of TYR and also has the potential to be employed to monitor TYR under normal physiological conditions (pH = 7.4, 37 °C).

To evaluate whether other substances can interfere with the detection of TYR under the optimal conditions, we next investigated the selectivity of probe **1** that treated with various interfering substances, such as inorganic salts (KCl, $MgCl_2$, $CaCl_2$, $FeCl_3$), sugars (glucose), vitamins (VB_6, VC), glycine, glutamic acid, cysteine, creatinine, urea, lipase, trypsin, catalase, and biologically relevant ROS (H_2O_2, TBHP, $ONOO^-$, ClO^-, ·OH, $^1O_2$, NO, NO_2^-). [12] The above results presented in Fig. S9 (ESI†), the probe signal that reacted with TYR was dramatically increased. Whereas the biological substances including ROS did not produce obvious fluorescence responses either. The data reported that the probe **1** had high selectivity to detect TYR without interference from other substances and excellent reliability in a complex biological environment. In addition, the binding ability of TYR with probe **1** was studied by a docking study. The docking score (-log K_d) is found to be 8.54, indicating a strong binding affinity between probe **1** and TYR. This is supported by the result of the ribbon model created by Pymol. As shown in Fig. 2B, the details of the binding of **1** to TYR domains showing five potential hydrogen bonds in yellow dotted lines.

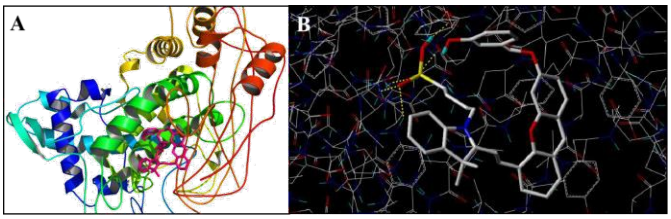

Fig. 2. (A) The docked conformer of probe **1** at the binding cleft of TYR (generated *via* Surflex docking-scoring combinations); (B) the details of the binding of probe **1** to TYR.

Based on the above conditional optimization, we carefully evaluated the sensitivity of the fluorescent response of the probe to different concentrations of TYR, as it is a key parameter for probe performance. As shown in Fig. 1B, an excellent linear correlation (R^2 = 0.9972) in the range from 10 to 70 μg/mL with a regression equation of ΔF =31.5 [TYR] (μg/mL) + 601.8. The detection limit for TYR was 0.11 μg mL^{-1} based on signal-to-noise ratio (S/N = 3). Furthermore, we compared probe **1** with some known TYR fluorescent probes in Electronic Supplementary Information (Table 1, ESI†).

To verify that the fluorescence enhancement was triggered by the reaction of probe and TYR. Kojic acid, as a standard inhibitor of TYR, was added to the reaction system that reveals 100 and 200 μM of kojic acid can inhibit the TYR activity, respectively.[13] As shown in Fig. S10 (ESI†), when kojic acid was added to the solution containing TYR and probe **1**, compared with the control group, the existence of kojic acid led to dramatic decrease of fluorescence intensity, and the fluorescence intensity decreased with the increase of the kojic acid concentration. At the same time, kojic acid has little effect on the fluorescence of both the fluorophore and probe **1** when TYR was absent. Therefore, the results indicate that the activity of TYR is inhibited by kojic acid, and the fluorescence change of probe **1** and TYR reaction is indeed caused by the cleavage reaction of the enzyme.

Before cell imaging, the biocompatibility of probe was evaluated by standard MTT assay, because cytotoxicity was an important aspect of biological imaging. The results were exhibited in Fig. S11 (ESI†), which showed that the probe and fluorophore had no significant toxicity to B16 cells at 37 °C for 24 h. Thus, the probe **1** had potential applications in living cell systems.

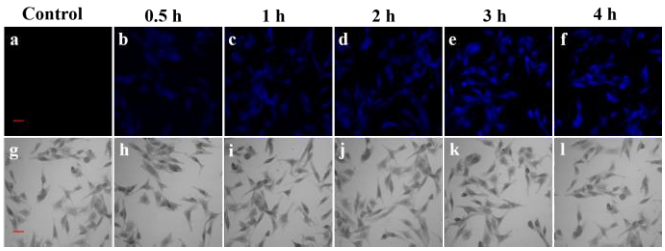

Fig. 3 Confocal fluorescence images of TYR in B16 cells at different times. (a) B16 cells only (control). Then the B16 cells were incubated with 10 μM probe **1** for (b) 0.5 h. (c) 1 h. (d) 2 h. (e) 3 h. (f) 4 h. The differential interference contrast (DIC) images of the corresponding samples are shown below (panels g–l). Scale bar: 20 μm.

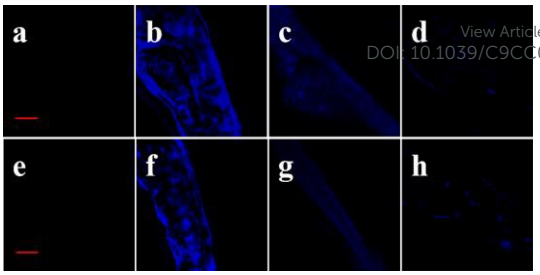

View Article Online
DOI: 10.1039/C9CC04714J

Fig. 4 Fluorescence images of TYR in living 3-day-old zebrafish (yolk sac and tail): (a, e) zebrafish only (control); (b, f) zebrafish treated with probe **1** (10 μM) for 3 h; (c, g) zebrafish were preincubated with 100 μM kojic acid for 1 h and treated with probe **1** (10 μM) for 3 h; (d, h) zebrafish were preincubated with 200 μM kojic acid for 1 h and treated with probe **1** (10 μM) for 3 h. Scale bar = 200 μm.

The combination of laser confocal and fluorescent probes makes it easier and more intuitive to detect TYR in biological systems. In view of the biopermeable and low cytotoxicity of probe **1**, we evaluated the response time of probe **1** to the TYR in living B16 cells. The fluorescence intensity of B16 cells that incubated with probe **1** (10 μM) was observed by confocal laser microscopy at 0 h, 0.5 h, 1 h, 2 h, 3 h, 4 h, respectively. The morphologies of the cells can be clearly observed in Fig. 3, the B16 cells were treated probe **1** for 0.5 h exhibited weak fluorescence. However, the fluorescence intensity of the cells gradually increased with time until the maximum intensity was reached at 3 h, and no significant fluorescence increase was observed at 4 h. As shown in Fig. S12 (ESI†), the fluorescence intensity of the B16 cells treated with 10 μM probe **1** for 0.5 h, 1 h, 2 h, 4 h decreased to ca.45%, ca.65% and ca.82%, ca.97% respectively, with respect to that treated with probe **1** for 3 h defined as 1.0. The observations indicated that the probe **1** can be applied for effective monitor intracellular TYR in living B16 cells.

In order to verify whether the fluorescence came from the reaction of probe **1** with TYR, we conducted the following kojic-acid-involved experiments. As displayed in Fig. S13 (ESI†), the cells treated with probe **1** that exhibit fluorescence that come from endogenous TYR in B16 cells. The fluorescence imaging of TYR in HepG2 cells (non-melanoma cell lines) was performed, almost no fluorescence was observed in HepG2 cells treated with probe **1**, because it was reported that TYR expression was mainly limited to melanocytes and was low in HepG2 cells.[14] As expected, the fluorescence of cells pretreated with kojic acid was significantly decreased. The relative pixel intensity measurements obtained from the images of cells were examined (Fig. S14, ESI†). The fluorescence intensity of the B16 cells treated with 10 μM probe **1** and 200 μM kojic acid decreased to ca.27%, the HepG2 cells treated with 10 μM probe **1** for 3 h decreased to ca.28%, with respect to that B16 cells treated with probe **1** for 3 h defined as 1.0. We can conclude that the fluorescence does come from the reaction of probe with TYR.

After proving the feasibility of probe **1** to track TYR in living cells, then we further paid more attention on whether probe **1** could be used for monitoring endogenous TYR in zebrafish. According to previous reports, zebrafish express high levels of TYR during embryonic period, after which TYR is dispersed throughout the body as the zebrafish grows.[15] As can be seen from the Fig. 4, the 3-day-old zebrafish without any treatment showed no fluorescence. However, after treated with 10 μM probe **1**, strong fluorescence was observed in the body of zebrafish. This implies that the probe is organism permeable and that zebrafish contain detectable levels of TYR. Then we did inhibitor experiments further proved that fluorescence came from the reaction between the probe **1** and TYR. The fluorescence intensity of zebrafish treated with kojic acid decreased obviously. The DIC images of the corresponding zebrafish and relative pixel intensity measurements obtained from the images of zebrafish were examined (Fig. S15 and S16, ESI†). The fluorescence intensity of the living 3-day-old zebrafish treated with 10 μM probe **1** and 100 μM kojic acid decreased to ca.48%, the zebrafish treated with 10 μM probe **1** and 200 μM kojic acid decreased to ca.27%, with respect to that zebrafish treated with probe **1** for 3 h (defined as 1.0). The results indicate that the probe **1** is capable of monitoring endogenous TYR in zebrafish.

To verify the ability of the probe **1** to detect melanoma in mouse, the tumor model was established by subcutaneous injection of melanoma cells (B16) in the right thigh of BALB/c nude mouse at the age of 5 weeks. The mouse was kept for about 2 weeks and then divided into two groups. Then live imaging of mouse was performed on small animal optical imaging system. We obtained images of mouse after injection of probe at 0, 60, 90, 120, 180 min, that given in Fig. 5. We can observe the weak fluorescence at the tumor site after 60 min of probe injection, indicating that the probe has good tissue permeability and high sensitivity. Within 180 min of monitoring, the fluorescence signal at tumor sites in mouse became more and more obvious over time. The relative pixel intensity measurements obtained from the images of mouse were examined (Fig. S17, ESI†). The fluorescence intensity of the mouse treated with probe **1** for 60 min, 90 min, 120 min decreased to ca.71%, ca.83%, ca.89%, with respect to that mouse treated with probe **1** for 180 min (defined as 1.0). The fluorescence intensity of the second group of mouse was pretreated with kojic acid (1 mM, 100 μL) for 60 min, and followed by injection of probe **1** (1 mM, 100 μL) for 60 min, 90 min, 120 min, 180 min decreased to ca.47%, ca.53%, ca.69%, ca.82%, with respect to that mouse treated with probe **1** for 180 min (defined as 1.0). A similar time course of fluorescent signal but 1.3-fold lower in intensity was obtained for mice pretreated with kojic acid. Compared with the mouse injected with probe **1** only, the

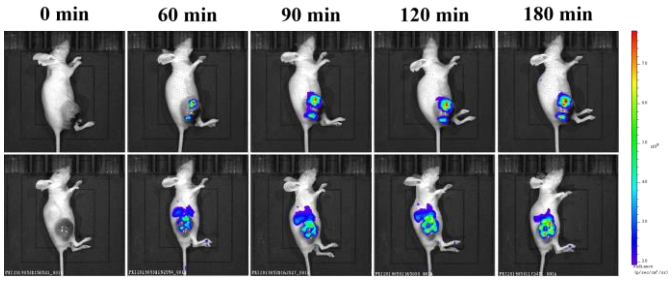

Fig. 5 Representative fluorescence images of BALB/c mouse (pseudocolor). The mouse received an intravenous injection of probe **1** (1 mM, 100 μL) at different times (0, 60, 90, 120, 180 min). The second group of mouse was pretreated with kojic acid (1 mM, 100 μL) for 60 min, and followed by injection of probe **1** (1 mM, 100 μL) into the same region at different times (0, 60, 90, 120, 180 min).

fluorescence intensity of the mouse pretreated with kojic acid and then injected with probe **1** was significantly weak, indicating that kojic acid effectively inhibited TYR. *In vivo* TYR imaging may be a promising method for early detection of malignant melanoma.

In summary, this paper reviews the synthesis of near-infrared fluorescent probes and their excellent properties, as well as their application in zebrafish *in vivo* and *in vitro* living cell imaging. The probe connected a new water-soluble fluorophore with a recognition group that could avoid ROS interference and specifically recognize TYR. The probe is highly stable over physiological temperature and pH ranges and is capable of accurately detecting TYR in biological systems without interference from ubiquitous entities. Especially, the probe has been successfully applied to the diagnosis of melanoma in a xenogeneic mouse model. It demonstrates favorable characteristics in terms of low toxicity, high specificity, high sensitivity, stable photo-stability. The superior properties of the probe make it of great potential use in other biosystems and *in vivo* imaging studies.

Conflicts of interest

There are no conflicts to declare.

Acknowledgements

We are grateful to the financial support from the National Natural Science Foundation of China (Nos.21605099), the Fundamental Research Funds for the Central Universities, China (GK201802019), and Shaanxi Province Agricultural Science and Technology Innovation and Key Project (2018NY-099). Financial support from the Young Talent Fund of University Association for Science and Technology in Shaanxi, China (20180207) is also greatly appreciated.

Notes and references

1 (*a*) M. U. A. Prathap, C. I. Rodriguez, O. Sadak, J. Guan, V. Setaluri and S. Gunasekaran, *Chem. Commun (Camb).*, 2018, **54**, 710-714; (*b*) C. Zhan, J. Cheng, B. Li, S. Huang, F. Zeng and S. Wu, *Anal. Chem.*, 2018, **90**, 8807-8815; (*c*) R. Seenivasan, N. Maddodi, V. Setaluri and S. Gunasekaran, *Biosensors. Bioelectronics*., 2015, **68**, 508-515.

2 (*a*) X. Wu, X. Li, H. Li, W. Shi and H. Ma, *Chem. Commun (Camb).*, 2017, **53**, 2443-2446; (*b*) H. Li, W. Liu, F. Zhang, X. Zhu, L. Huang and H. Zhang, *Analz. Chem.*, 2018, **90**, 855-858; (*c*) E. Solem, F. Tuczek and H. Decker, *Angew. Chem. Int. Edit.*, 2016, **55**, 2884-2888; (*d*) C. Bochot, A. Gouron, L. Bubacco, A. Milet, C. Philouze, M. Reglier, G. Serratrice, H. Jamet and C. Belle, *Chem. Commun (Camb).*, 2014, **50**, 308-310.

3 (*a*) X. Li, W. Shi, S. Chen, J. Jia, H. Ma and O. S. Wolfbeis, *Chem. Commun (Camb).*, 2010, **46**, 2560-2562; (*b*) H. Ao, Z. Qian, Y. Zhu, M. Zhao, C. Tang, Y. Huang, H. Feng and A. Wang, *Biosens. Bioelectron.*, 2016, **86**, 542-547; (*c*) J. Zhou, W. Shi, L. Li, Q. Gong, X. Wu, X. Li and H. Ma, *Anal. Chem.*, 2016, **88**, 4557-4564.

4 (*a*) Z. Li, Y. F. Wang, X. Zhang, C. Zeng, L. Hu and X. J. Liang, *Biosens. Bioelectron.*, 2017, **242**, 189-194; (*b*) X. Yan, H. Li, W. Zheng and X. Su, *Anal. Chem.*, 2015, **87**, 8904-8909; (*c*) T. I. Kim, J. Park, S. Park, Y. Choi and Y. Kim, *Chem. Commun (Camb).*, 2011.**47**,12640-12642.

5 (*a*) H. B. Yildiz, R. Freeman, R. Gill and I. Willner, 2008. *Anal. Chem*., 2008, **80**, 2811-2816; (*b*) R. F. Boyer, *J. Chem. Educ*., 1977, **54**, 585-586; (*c*) J. C. Espin, M. Morales, R. Varón, J. Tudela and F. Garcia-Canovas, J. Food. Sci. 1996, **61**, 1177-1182; (*d*) J. Wei, J. Qiu, L. Li, L. Ren, X. Zhang, J. Chaudhuri and S. Wang, *Nanotechnology*., 2012, **23**, 335707; (*e*) S. Li, L. Mao, Y. Tian, J. Wang and N. Zhou, *Analyst*, 2012, **137**, 823-825; (*f*) R. Freeman, J. Elbaz, R. Gill, M. Zayats and I. Willner, *Chem-Eur. J*., 2007, **13**, 7288-7293.

6 (*a*) D. Li, R. Gill, R. Freeman and I. Willner, *Chem. Commun (Camb).*, 2006, **48**, 5027-5029; (*b*) R. Baron, M. Zayats and I. Willner, *Anal. Chem.*, 2005, **77**, 1566-1571.

7 (*a*) Y. Teng, X. Jia, J. Li and E. Wang, *Anal. Chem.*, 2015, **87**, 4897-4902; (*b*) J. Sun, H. Mei, S. Wang and F. Gao, *Anal. Chem.*, 2016, **88**, 7372-7377; (*c*) S. Li, R. Hu, S. Wang, X. Guo, Y. Zeng, Y. Li and G. Yang, *Anal. Chem.*, 2018, **90**, 9296-9300.

8 (*a*) W. Chen, S. Xu, J. J. Day, D. Wang and M. Xian, *Angew. Chem. Int. Ed*., 2017, **56**, 16611-16615; (*b*) Y. Fang, W. Chen, W. Shi, H. Li, M. Xian and H. Ma, *Chem. Commun (Camb).*, 2017, **53**, 8759-8762; (*c*) J. Zhang, X. Zhen, J. Zeng and K. Pu, *Anal. Chem.*, 2018, **90**, 9301-9307. (*d*) M. Peng, Y. Wang, Q. Fu, F. Sun, N. Na and J. Ouyang, *Anal. Chem.*, 2018, **90**, 6206-6213. (*e*) X. W. Tian, Z. Li, Y. Sun, Wang, P. Wang, H. M. Ma, *Anal. Chem.*, 2018, **90**, 13759-13766.

9 (*a*) J. Kim and Y. Kim, *Analyst*, 2014, **139**, 2986-2989; (*b*) W. Zhang, P. Li, F. Yang, X. Hu, C. Sun, W. Zhang, D. Chen and B. Tang, *J. Am. Chem. Soc.*, 2013, **135**, 14956-14959; (*c*) H. Zhang, J. Liu, Y. Q. Sun, Y. Huo, Y. Li, W. Liu, X. Wu, N. Zhu, Y. Shi and W. Guo, *Chem. Commun (Camb).*, 2015, **51**, 2721-2724.

10 X. Wu, L. Li, W. Shi, Q. Gong and H. Ma, *Angew. Chem. Int. Edit.*, 2016, **55**, 14728-14732.

11 (*a*) D. Li, Z. Li, W. Chen and X. Yang, *J. Agr. Food. Chem.*, 2017, **65**, 4209-4215; (*b*) K. Liu, H. Shang, X. Kong, M. Ren, J. Y. Wang, Y. Liu and W. Lin, *Biomaterials*, 2016, **100**, 162-171; (*c*) J. Hou, M. Qian, H. Zhao, Y. Li, Y. Liao, G. Han, Z. Xu, F. Wang, Y. Song and Y. Liu, *Anal. Chim. Acta.*, 2018, **1024**, 169-176; (*d*) X. Liu, H. Tian, L. Yang, Y. Su, M. Guo and X. Song, *Biosens. Bioelectron.*, 2018, **255**, 1160-1165.

12 W. Chen, A. Pacheco, Y. Takano, J. J. Day, K. Hanaoka and M. Xian., *Angew. Chem. Int. Ed*., 2016, **55**, 9993-9996.

13 T. S. Chang, Int. *J. Mol. Sci*., 2009, **10**, 2440-2475.

14 A. M. Jordan, T. H. Khan, H. Malkin, H. M. I. Osborn, *Bioorg. Med. Chem*., 2002, **10**, 2625-2633.

15 E. Camp, M. Lardelli, *Dev. Genes. Evol*., 2001, **211**, 150-153.